Submitted July 2003

Numerical Modeling of Microwave Testing of Materials Using a Transmission Line Matrix Technique

by Razvan Ciocan* and Nathan Ida†

ABSTRACT

A three dimensional transmission line matrix model was developed to simulate microwave investigation of materials. A transmission line matrix algorithm that allows the simulation of the real microwave probe scanning was developed. Numerical modeling was carried out for frequencies that are commonly used in microwave nondestructive testing (NDT). Structures with local discontinuities in the electric permittivity are modeled numerically. The excitation parameters used in the numerical modeling of scanning microwave microscopy were determined based on an initial frequency experimental response obtained from a plate with known permittivity. The numerical model developed in this paper is based on the symmetric condensed node. Experimental data obtained by the authors are used to validate the numerical models presented in this work. The model developed and described in this paper has proven its viability, giving accurate results when compared to analytical solutions where these solutions are available and when compared to experimental results obtained for geometries that do not allow an analytical solution.

Keywords: *microwave microscopy, NDT, transmission line matrix, numerical modeling.*

INTRODUCTION

The interest in using microwaves for nondestructive testing (NDT) has increased constantly in past years. Maxwell's equations give a fully theoretical description of electromagnetic scattering. Unfortunately, their analytical solutions are available for just a few particular cases. To improve the results obtained in the NDT of materials, considerable theoretical effort is invested in developing reliable mathematical models of wave propagation in different media. Due to the complexity of the problems, numerical methods have proven to be an adequate approach; hence, they are intricately associated with the development of NDT methods.

The first book that proposed a numerical model for microwave nondestructive testing was published in 1992 (Ida, 1992). Three years later, a book was dedicated exclusively to modeling electromagnetic NDT (Ida, 1995). The book offers a comprehensive treatment of finite difference and finite element methods. A special chapter is also dedicated to the method of moments. This last method was used to model the detection of developing cracks using microwave techniques (Zoughi, 2000). The numerical methods that are most commonly used in NDT are: method of moments; finite element; and finite difference time domain.

Applying the method of moments, one needs to divide a finite volume into elements or cells and define appropriate basis and weighting functions. The first three dimensional method of moments model for electromagnetic scattering by a heterogeneous dielectric scatterer was reported in 1974 (Livesay and Chen, 1974). A very serious limitation of the method of moments is the need to invert a complex, very large matrix. This process should be repeated for each frequency of interest. Another important limitation of the method is related to singularities that need to be resolved each time one defines a new basis function. The finite element method is not limited by geometric shapes and it is a powerful method for handling inhomogeneities and anisotropies. The method was applied with limited success to unbounded systems (Chadwick et al., 1999). A specific limitation for this method is related to the occurrence of "spurious" modes (solutions with no physical meaning that appear in numerical modeling). As one increases the mesh refinement to improve the accuracy of a solution, the number of spurious solutions also increases. The most frequently used numerical method in the time domain is finite difference time domain. The method was first proposed in 1966 (Yee, 1966) and involves transformation of differential equations in difference equations. The main advantage of the method is that the difference equations can be solved in a step by step time scheme as long as a certain stability requirement is satisfied. In Yee's scheme, the electric and magnetic field components are computed at alternate time steps and at half space increments. This is the main difference between a finite difference time domain and a transmission line matrix scheme based on the symmetrical condensed node. The immediate benefit of having all field components at the same point consists in modeling space discontinuities.

The transmission line matrix technique is relatively new to the large family of numerical methods. The first time the transmission line matrix technique appeared in an article was in September of 1971 (Johns and Beurle, 1971). Paul Johns, the first author of this article, is considered to be the creator of the method. His articles demonstrated that transmission line matrices could be used in a wide range of applications. A treatment of bidimensional lossy waveguides using this method was proposed three years later (Akhtarzad and Johns, 1974). The rationale for using the scattering matrix to describe inhomogeneous two dimensional waveguide problems was introduced by Johns (1974) and it was exemplified for a waveguide with dielectric ridge. A three dimensional model was first proposed in 1975 (Akhtarzad and Johns, 1975). The validity of the transmission line matrix model is demonstrated in this article by computing the resonance frequencies for rectangular cavities loaded with dielectric slabs. Lumped network models of Maxwell's equations were the first basic formulations of the transmission line matrix technique. Based on this formulation, large structures are divided into substructures for which models are developed separately (Brewitt-Taylor and Johns, 1980). Then the whole network response is obtained by assembling together all the substructures. This method was called diakoptics (Braemeller and John, 1969) and was extensively used in transmission line matrix

* Department of Physics and Astronomy, College of Science and Engineering, Clemson University, 118 Kinard Laboratory of Physics, Box 340978, Clemson, SC 29634-0978; (864) 656-5317; fax (864) 656-0805; e-mail <ciocan@clemson.edu>.

† Department of Electrical and Computer Engineering, University of Akron, Akron, OH 44325-3904; fax (330) 972-6487; e-mail <ida@uakron.edu>.

modeling (Hoefer and So, 1993). A comprehensive treatment of the transmission line matrix models for materials with nonlinear properties was published by Paul and Christopoulos (2002). A significant development in the three dimensional transmission line matrix was made by the introduction of the symmetrical condensed node (Johns, 1986). When this node was introduced, it was a purely algebraic construction. It was shown that this type of node accommodates both forms of scattering matrices — for lossless and lossy materials (Johns, 1987). Almost 30 years after the first article was published, the method is considered to be "a modeling process rather than a numerical method for solving differential equations" (Sadiku and Obiozor, 2000). The method is a direct numerical implementation of the Huygen's principle (Kagawa et al., 1998). The wave front corresponding to each iteration (instant in time) for a certain point in space is a result of the waveforms generated at neighboring points in the previous iteration. The transmission line matrix requires the division of the solution region into a rectangular mesh of transmission lines. The nodes of the mesh are points of discontinuity for impedances. To solve a problem using the transmission line matrix, a set of boundary conditions and material parameters must be provided. An initial excitation, called input, must also be given. Then the impulses are propagated throughout the mesh using the scattering theory on the transmission lines. There is no limitation regarding the frequency of interest, but the size of the mesh imposes an upper limit on the frequency response analysis.

The transmission line matrix algorithm has high flexibility in dealing with various types of input signals and boundaries. These advantages can be exploited for NDT in several ways:

- a real digitized signal (for example, a signal that comes from a data acquisition board) can be used as an input signal in a transmission line matrix model
- complex boundary geometries can be introduced in the numerical model regardless of the algorithm convergence
- the transmission line matrix technique offers a versatile tool to reconstruct the initial signal based on the real digitized signal for homogeneous media
- the transmission line matrix technique can easily generate a time or frequency domain signal for a supposedly known configuration.

Based on this, a multilayer structure can be fully characterized using an iterative process. The material parameters of the multilayer structure under investigation can be changed in the transmission line matrix model, so that the numerically generated signal fits the real signal.

Based on the above considerations, we propose the application of a transmission line matrix for microwave NDT. The following sections of this paper show how the transmission line matrix models for microwave NDT were developed, implemented and validated on experimental data obtained by the authors.

TRANSMISSION LINE MATRIX ALGORITHM RATIONALE

The name of the algorithm comes from the equivalence that exists between the wave equation for electric and magnetic fields in free space and wave equations for voltages and currents in a transmission line. Considering Kirchhoff's laws for a shunt transmission line (lossless and nondispersive) the wave equation for the voltage can be written (Ida. 2000):

(1) $$\frac{\partial^2 V}{\partial x^2}+\frac{\partial^2 V}{\partial y^2}=2CL\frac{\partial^2 V}{\partial t^2}$$

The elements of the circuit (L and C) are chosen to model the propagation in a homogenous infinite space with impedance Z_0. Based on Maxwell's equations, the wave equation for transverse magnetic waves in a source free region for nondispersive media can be written as (Ida. 2000):

(2) $$\frac{\partial^2 E_z}{\partial x^2}+\frac{\partial^2 E_z}{\partial t^2}$$

Given the equivalence between the wave equation written for acoustic or electromagnetic waves and the wave equation for an ideal transmission line, scattering matrix theory is applied to study the equivalent microwave network system as seen at its ports. The scanning matrix theory determines the output at all ports for a given input. In a general form this can be written as:

(3) $$\left[{}_nV^r\right]=[S]\left[{}_nV^i\right]$$

where

$[V^r]$ = the matrix of reflected pulses at instant n
$[V^i]$ = the matrix of incident pulses at instant n
$[S]$ = the scattering matrix.

These pulses are defined in Figure 1. The transmission line matrix equations for the field components are written using the voltages on the node edges. The three index notation used in this paper (Figure 1) is related to the position of the ports and to the direction of link lines. For example, V_{xpy} is the voltage pulse on a link line parallel to the X axis (x index), on the positive side (p index) and polarized in the Y direction (y index). A full derivation for the scattering matrix elements starting from Maxwell equations was obtained (Ciocan, 2003). The elements of the scattering matrix are depicted in Table 1 and are obtained in such a way that charge and flux conservation laws are obeyed for the node. As an example, a component of the reflected voltage from Equation 3 is obtained using scattering matrix elements given in Table 1 as:

(4) $$\begin{aligned}{}_nV^r_{xpy} = &-{}_nV^i_{ynx}d_{xy}+{}_nV^i_{xny}c_{xy}+{}_nV^i_{zny}b_{xy}+{}_nV^i_{zpy}b_{xy}\\ &+{}_nV^i_{xpy}a_{xy}+{}_nV^i_{ypx}d_{xy}+{}_nV^i_{ocy}g_y+{}_nV^i_{scz}i_{xy}\end{aligned}$$

In Equation 4, the coefficients of the voltages are extracted from Table 1 and are given by:

(5) $$d_{xy}=\frac{2}{Z_z+4+g_{mz}}$$

(6) $$c_{xy}=\frac{Y_y-g_{ey}}{2\left(Y_y+4+g_{ey}\right)}-\frac{Z_z+g_{mz}}{2\left(Z_z+4+g_{mz}\right)}$$

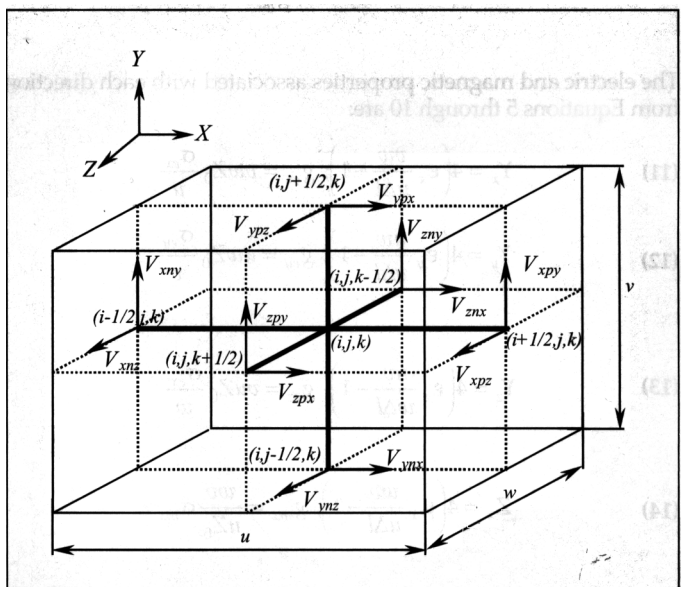

Figure 1 — Symmetrical condensed nodes for a parallelepipedic region of space with dimensions u, v *and* w.

Table 1 Scattering matrix elements and voltage correspondence between three index (top row and last column) and classical (Johns, 1987) notations (second row and penultimate column)

V_{ynx}	V_{znx}	V_{xny}	V_{zny}	V_{ynz}	V_{xnz}	V_{ypz}	V_{zpy}	V_{zpx}	V_{xpz}	V_{xpy}	V_{ypx}	V_{scx}	V_{scy}	V_{scz}	V_{ocx}	V_{ocy}	V_{ocz}		
1	2	3	4	5	6	7	8	9	10	11	12	13	14	15	16	17	18		
a_{yx}	b_{yx}	d_{yx}						b_{yx}		$-d_{yx}$	c_{yx}	g_x					i_{yx}	1	V_{ynx}
b_{zx}	a_{zx}				d_{zx}			c_{zx}	$-d_{zx}$	0	b_{zx}	g_x						2	V_{znx}
d_{xy}		a_{xy}	b_{xy}				b_{xy}			c_{xy}	$-d_{xy}$		g_y					3	V_{xny}
		b_{zy}	a_{zy}	d_{zy}		$-d_{zy}$	c_{zy}			b_{zy}			g_y		i_{zy}			4	V_{zny}
			d_{yz}	a_{yz}	b_{yz}	c_{yz}	$-d_{yz}$		b_{yz}					g_z	$-i_{yz}$			5	V_{ynz}
	d_{xz}			b_{xz}	a_{xz}	b_{xz}		$-d_{xz}$	c_{xz}					g_z				6	V_{xnz}
			$-d_{yz}$	c_{yz}	b_{yz}	a_{yz}	d_{yz}		b_{yz}					g_z	i_{yz}			7	V_{ypz}
		b_{zy}	c_{zy}	$-d_{zy}$		d_{zy}	a_{zy}			b_{zy}			g_y		$-i_{zy}$			8	V_{zpy}
b_{zx}	c_{zx}				$-d_{zx}$			a_{zx}	d_{zx}		b_{zx}	g_x				i_{zx}		9	V_{zpx}
	$-d_{xz}$			b_{xz}	c_{xz}	b_{xz}		d_{xz}	a_{xz}					g_z		$-i_{xz}$		10	V_{xpz}
$-d_{xy}$		c_{xy}	b_{xy}				b_{xy}			a_{xy}	d_{xy}		g_y				i_{xy}	11	V_{xpy}
c_{yx}	b_{yx}	$-d_{vx}$						b_{yx}		d_{vx}	a_{yx}	g_x					$-i_{yx}$	12	V_{ypx}
e_{yx}	e_{zx}							e_{zx}			e_{yx}	h_x						13	V_{scx}
		e_{xv}	e_{zv}				e_{zv}			e_{xy}			h_y					14	V_{scy}
				e_{yz}	e_{xz}	e_{yz}			e_{xz}					h_z				15	V_{scz}
			f_v	$-f_x$		f_x	$-f_x$											16	V_{ocx}
	$-f_z$				f_y			f_v	$-f_y$							l_y		17	V_{ocy}
f_z		$-f_z$								f_z	$-f_z$							18	V_{ocz}

(7) $$b_{xy} = \frac{2}{Y_y + 4 + g_{ey}}$$

(8) $$a_{xv} = \left| \frac{2}{Y_y + 4 + g_{ey}} \quad \frac{2}{Z_z + 4 + g_{mz}} \right.$$

(9) $$g_y = \frac{2\sqrt{Y_y}}{Y_y + 4 + g_{ey}}$$

(10) $$i_{xy} = \frac{2}{Z_z + 4 + g_{mz}}$$

The electric and magnetic properties associated with each direction from Equations 5 through 10 are:

(11) $$Y_x = 4\left(\varepsilon_x \frac{vw}{u\Delta l} \right), \quad g_{ex} = vwZ_0 \frac{\sigma_{ex}}{u}$$

(12) $$Y_y = 4\left(\varepsilon_y \frac{uw}{v\Delta l} - 1 \right), \quad g_{ey} = uwZ_0 \frac{\sigma_{ey}}{v}$$

(13) $$Y_z = 4\left(\varepsilon_z \frac{uv}{w\Delta l} - 1 \right), \quad g_{ez} = vuZ_0 \frac{\sigma_{ex}}{w}$$

(14) $$Z_x = 4\left(\mu_x \frac{wv}{u\Delta l} - 1 \right) \quad \frac{wv}{uZ_0}\sigma_{mx}$$

(15) $$Z_y = 4\left(\mu_y \frac{wu}{v\Delta l} - 1 \right), \quad g_{my} \quad \frac{uw}{vZ_0}\sigma_{my}$$

(16) $$Z_z = 4\left(\mu_z \frac{uv}{w\Delta l} - 1 \right), \quad g_{mz} = \frac{uv}{wZ_0}\sigma_{mz}$$

Equations 11 through 16 define the material parameters that are used in the definition of scattering matrix elements. The quantities defined in them are associated to each of the axes X, Y and Z using the generic index *i*: Y_i = characteristic admittance; Z_i = characteristic impedance; g_{ei} = electric conductance; g_{mi} = magnetic conductance. The previous quantities are defined as functions of local material properties associated to axis *i* (permittivity, e_i; permeability, m_i; electric conductivity, σ_{ei}; and magnetic conductivity, σ_{mi}) and the node dimensions *u*, *v* and *w*, defined in Figure 1. In Equations 11 through 16, Δl is the minimum value of all the node dimensions throughout the mesh.

The field components at the moment *n* can be written in terms of incident voltages as follows (Ciocan, 2003):

(17) $$ {}_nE_x(i,j,k) = \frac{2\left({}_nV^i_{ypx} + {}_nV^i_{ynx} + {}_nV^i_{zpx} + {}_nV^i_{znx} + {}_nV^i_{ocx}\sqrt{Y_x} \right)}{\left(Y_x + 4 + g_{ex} \right)} $$

(18) $$ {}_nE_y(i,j,k) = \frac{2\left({}_nV^i_{zpy} + {}_nV^i_{zny} + {}_nV^i_{xpy} + {}_nV^i_{xny} + \sqrt{Y_y}\,{}_nV^i_{ocy} \right)}{\left(Y_y + 4 + g_{ey} \right)} $$

(19) $$ {}_nE_z(i,j,k) = \frac{2\left({}_nV^i_{ypz} + {}_nV^i_{ynz} + {}_nV^i_{xpz} + {}_nV^i_{xnz} + \sqrt{Y_z}\,{}_nV^i_{ocz} \right)}{\left(Y_z + 4 + g_{ez} \right)} $$

(20) $$ {}_nH_x(i,j,k) = \frac{2\left({}_nV^i_{zny} + {}_nV^i_{ypz} - {}_nV^i_{zpy} - {}_nV^i_{ynz} + \sqrt{Z_x}\,{}_nV^i_{scx} \right)}{\left(Z_x + 4 + g_{mx} \right)} $$

(21) $$ {}_nH_y(i,j,k) = \frac{2\left({}_nV^i_{zpx} - {}_nV^i_{xpz} - {}_nV^i_{znx} + {}_nV^i_{xnz} + \sqrt{Z_y}\,{}_nV^i_{scy} \right)}{\left(Z_y + 4 + g_{my} \right)} $$

(22) $$ {}_nH_z(i,j,k) = -\frac{2\left({}_nV^i_{xpy} - {}_nV^i_{ypx} - {}_nV^i_{xmy} + {}_nV^i_{ynx} + \sqrt{Z_z}\,{}_nV^i_{scz} \right)}{\left(Z_z + 4 + g_{mz} \right)} $$

The numerical implementation of a desired model is performed in three steps: preprocessing, computation and postprocessing (Figure 2). The preprocessing step includes determining the excitation signal parameters and generating the boundary coordinates of complex geometries. The processing step is made by the transmission line matrix algorithm. The main steps of this algorithm are: initialization, scattering and connection. The connection process is based on the fact that the reflected pulse for a certain node at $(k+1)\Delta t$ becomes the incident pulse for the neighboring nodes at the same moment, $(k+1)\Delta t$. Relations that describe the connection process can be written in an intuitive form using the three index notation (Figure 1). For example, the equations that model connection in the Y direction at instant $k+1$ are:

$$(23) \qquad {}_{k+1}V^{i}_{ynx}(x, y+1, z) = {}_{k+1}V^{r}_{ypx}(x, y, z)$$

$$(24) \qquad {}_{k+1}V^{i}_{ypx}(x, y-1, z) = {}_{k+1}V^{r}_{ynx}(x, y, z)$$

$$(25) \qquad {}_{k+1}V^{i}_{ynz}(x, y+1, z) = {}_{k+1}V^{r}_{ypz}(x, y, z)$$

$$(26) \qquad {}_{k+1}V^{i}_{ypz}(x, y-1, z) = {}_{k+1}V^{r}_{ynz}(x, y, z)$$

The scanning step was implemented. This step involves changing the position of excitation according to the experimental scanning pattern, whereby the transmission line matrix algorithm is repeated for each new position. The time response for each position is saved in an output file for further processing.

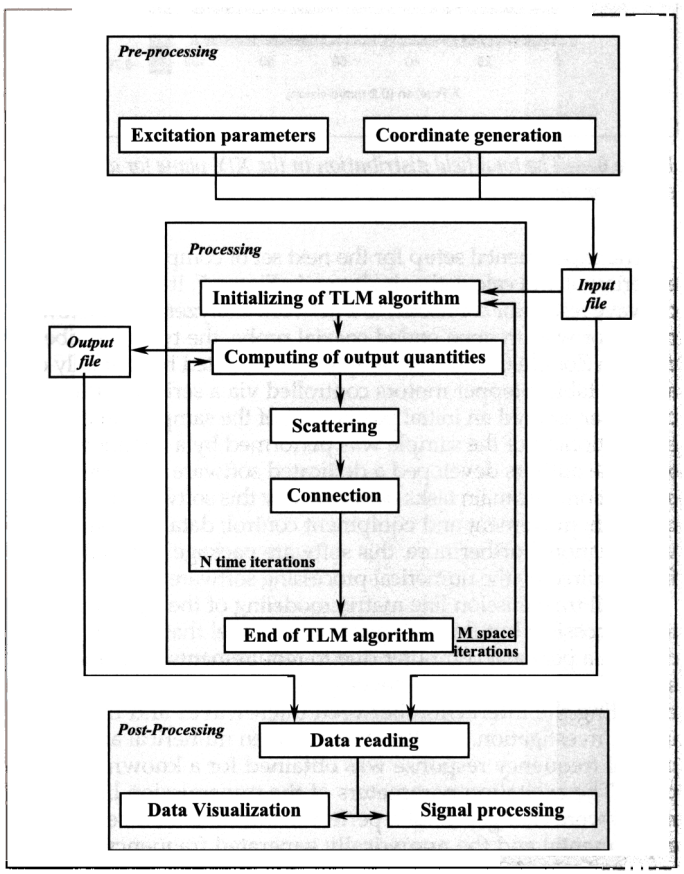

Figure 2 — Program structure for numerical implementation of transmission line matrix (TLM) models for microwave NDT.

The programs developed for the postprocessing part perform the following tasks:

- reading the data input files generated by the processing program
- data visualization in two or three dimensions for each iteration considered
- signal processing of the numerically generated signal in the time and frequency domains.

NUMERICAL MODEL VALIDATION

In order to demonstrate the transmission line matrix algorithm capability being used in NDT, some experiments were performed. All geometries considered belong to the "reflector with sharp edges" class. For this type of reflector, the analytical solutions are not available and other numerical methods (as presented in the introduction of this paper) can generate solutions with no physical meaning (spurious solutions).

This is not the case for the transmission line matrix algorithm. The formulation of a transmission line matrix algorithm can solve (provide a correct solution) for any type of configuration source reflector. These facts are illustrated below for three configurations that can be considered as fundamental for a numerical simulation of the NDT process. These configurations are: a pulsating source in front of a square; a sinusoidal source in front of a material with a small circular discontinuity on it; and a sinusoidal source in front of a material with two rectangular discontinuities on it. Based on these general configurations, all NDT problems encountered in real life can be numerically modeled. There is a single conceptual limitation of transmission line matrix models. The mesh size of these models should be less than one tenth of a wavelength ($\lambda/10$). This limit is related to the validity of transmission line matrix theory. For microwave frequencies, the $\lambda/10$ limit is not a problem. This means that practically any microwave NDT configuration can be transmission line matrix modeled. How the numerical model proposed deals with the objects with sharp edges is shown in Figure 3. A gaussian pulse was launched from the center of a mesh. The interaction of this wave with a perfectly reflecting square is shown for two iterations in a pseudo three dimensional representation. The first iteration shown corresponds to the instant when the wave front touches the square. The second iteration was chosen when the wave is propagating along the square edges. At this instant, a circular wave front was recomposed, as is shown by its projection on the X/Y plane and this is the wave front that will be received by a receiver that is placed in the same position where the transmitter was.

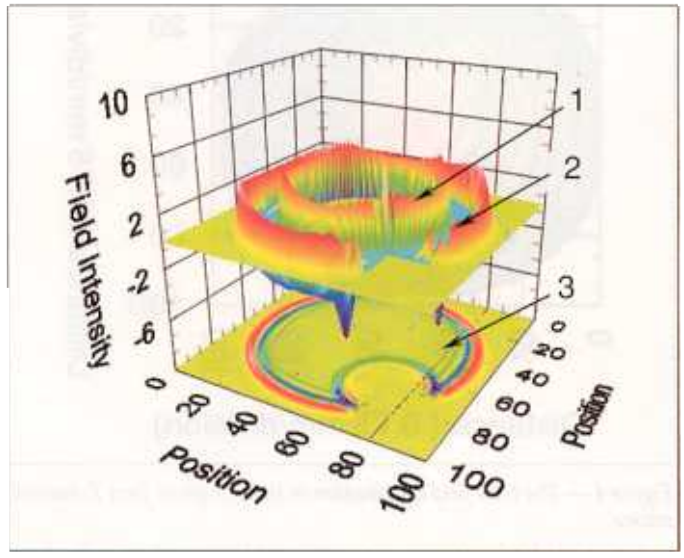

Figure 3 — The simulated waveforms for a gaussian wave reflection from a perfectly reflecting square: 1 is where the waveform touches the corner placed in position; 2 shows where the waveform is propagating along the square edges; 3 is an xy projection of the situation depicted in 2.

The quantitative comparison between the proposed numerical model and the analytical results was performed for the case where exactly analytical solutions are available (the perfectly conducting cube). The exact resonance frequencies can be computed in this case using the formula (Ida, 2000):

$$f_{mnp} = \frac{1}{2\sqrt{\mu\varepsilon}}\sqrt{\left(\frac{m}{a}\right)^2 + \left(\frac{n}{b}\right)^2 + \left(\frac{p}{d}\right)^2} \quad (27)$$

The three dimensional transmission line matrix model for a perfectly conducting cube 1 m (39 in.) on each side was implemented in a 50 by 50 by 50 mesh. The source was an x polarized E field and it was located in the center of the cube at the mesh point (25, 25, 25). A comparison between the computed frequencies and those obtained numerically is shown in Table 2. The results in this table show that the proposed numerical model can correctly predict the frequency response. In addition to that, the transmission line matrix models can correctly predict the electrical field distribution for three dimensional structures.

Table 2 The analytical and transmission line matrix frequencies for the dominant modes in a cubic cavity

Mode	Theoretical Frequency	Transmission Line Matrix Computed Frequency
TM110	212 MHz	212 MHz
TM120	335 MHz	335 MHz
TM220	424 MHz	423 MHz
TM310	475 MHz	475 MHz
TM320	541 MHz	540 MHz
TM330	636 MHz	636 MHz

Let us consider a small Z directed dipole fed with a sinusoidal signal at 20 GHz, positioned in front of a perfect conductor screen (a square 5.25 mm [0.2 in.] on each side) that is placed in the X/Y plane. There is a small hole (0.75 mm [0.03 in.]) in the center of this metalic screen. Figure 4 shows a Y/Z section of the total field distribution (in decibals). The representation in Figure 4 demonstrates that the transmission line matrix model proposed here can solve the field distribution for a rather complex structure, with a resolution better than $\lambda/20$ (mesh size for these simulations).

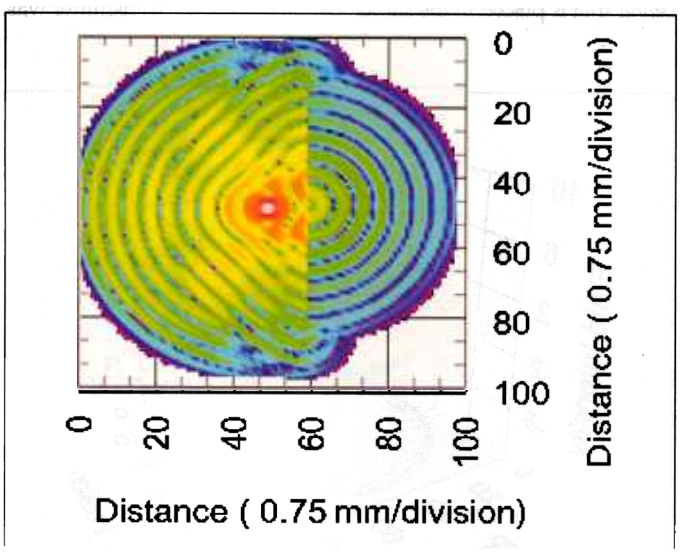

Figure 4 — The total field distribution in the Y/Z plane for a Z directed source.

Next, the field distribution for a more complicated structure was investigated numerically. The structure consisted of three identical metallic boxes (1.2 by 0.8 by 0.4 mm [0.05 by 0.03 by 0.02 in.]), A, B and C, situated in a free space. The distance between boxes A and B was 0.2 mm (7.9×10^{-3} in.) and that between boxes B and C was 0.8 mm (0.03 in.). A sinusoidal source was placed in front of box B, 1 mm (0.04 in.) away. The arrangement used in this case is shown in Figure 5. The source frequency was 1 GHz and its length was 0.9 mm (0.035 in.). The configuration investigated was one with a z directed source. The electrical field distribution for this configuration is given in Figure 6. The field distribution from this figure shows the transmission line matrix model proposed can accurately simulate the electrical field distribution associated with a relatively complicated geometry of both source and reflector.

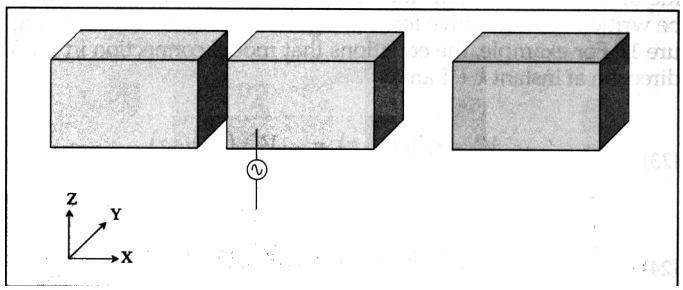

Figure 5 — The structure for which the electric field distributions are shown in Figure 6.

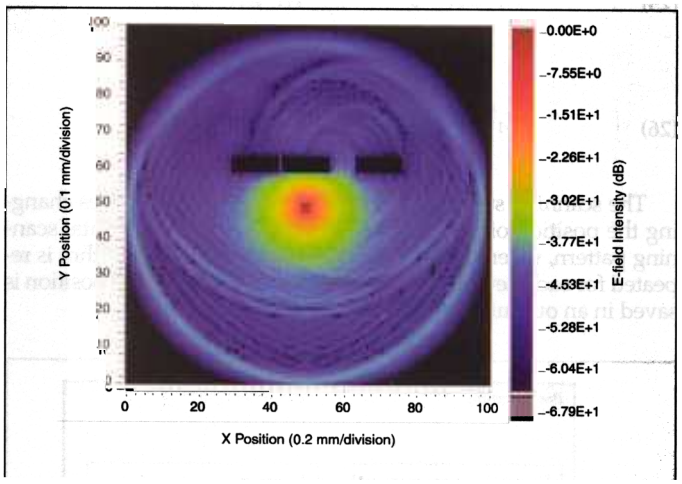

Figure 6 — The total field distribution in the X/Y plane for a Z directed source for the structure shown in Figure 5.

The experimental setup for the next set of comparisons between experiment and calculation is shown in Figure 7. It consists of a microwave resonator connected to a network analyzer. The microwave resonator was an open ended coaxial probe, the type described in detail in Zoughi (2000). The sample was mounted horizontally over an X/Y table. Stepper motors controlled via a serial interface by a computer assured an initial positioning of the sample. An extra micropositioning of the sample was performed by a commercial system. The authors developed a dedicated software package for this application. The main tasks performed by this software are: data acquisition; movement and equipment control; data processing; and visualization. Furthermore, this software package writes the input files required by the numerical processing software.

A full transmission line matrix modeling of the microwave system is possible but this will generate a model that cannot be handled on a personal computer due to requirements of memory and speed. The actual models developed in this work concentrate on modeling the interaction between microwaves and the sample under investigation. A calibration between numerical and experimental frequency response was obtained for a known dielectric plate. The excitation parameters of the transmission line matrix model were changed until a perfect fit was obtained between the experimental and the numerically generated frequency response curves obtained for a known microwave dielectric sample geometry. The excitation parameters determined in this way were used in the subsequent numerical simulations.

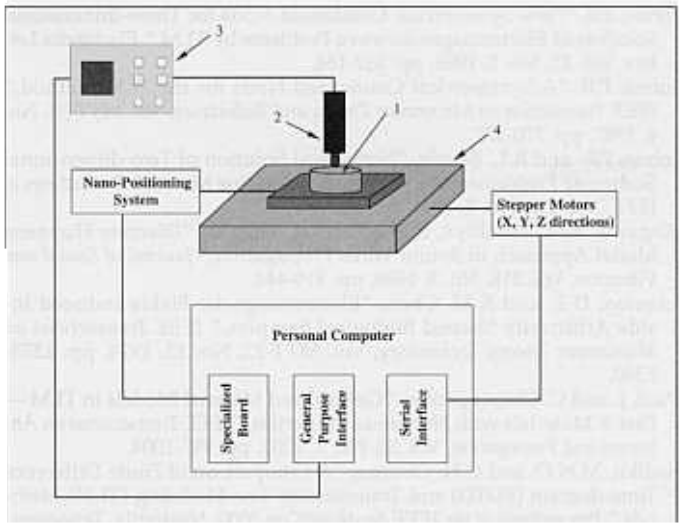

Figure 7 — Experimental setup used to validate the numerical models: 1 is the sample, 2 is the microwave probe, 3 is the network analyzer and 4 is the sample holder.

The quantity used to obtain a microwave image is S_{11}. This parameter cannot be obtained directly from the transmission line matrix algorithm because an incident field cannot be separated. To solve this problem, two successive runs of the program are needed. The first run is performed with the excitation without a reflecting object. This run will provide data for the reference port. A second run of the program will be performed considering the boundary conditions for the objects to be investigated. The S_{11} parameter is given by:

$$S_{11} = \frac{F_i - F_0}{F_i + F_0} \quad (28)$$

Here,

F_0 = the frequency response obtained for the same position of the excitation source without a reflecting object

F_i = the frequency response obtained for the same position of the excitation source with a reflector.

Figure 8 shows the plot of the S_{11} parameter for three different materials: metal, phenol-formaldehyde plastic ($\varepsilon_r = 5$) and polytetrafluoroethylene resin ($\varepsilon_r = 2$). The plot demonstrates the capability of the proposed transmission line matrix model to differentiate between materials with different electric permittivities. The frequency response was obtained after two intermediary signal processing steps — filtering and windowing. The same signal processing method was applied to the reference and reflected signals. Figure 9 shows the numerical results for the simulation of the scanning over two small pieces of phenol-formaldehyde plastic and polytetrafluoroethylene resin, respectively. Two rectangular (1.6 by 3 mm [0.06 by 0.1 in.]) dielectric pieces were investigated and the step size in scanning was 0.03 mm (1.3×10^{-3} in.). The dielectric profiles were obtained by selecting the corresponding computed S_{11} values for 1.72 GHz. This procedure is identical to that used in experimental microwave NDT.

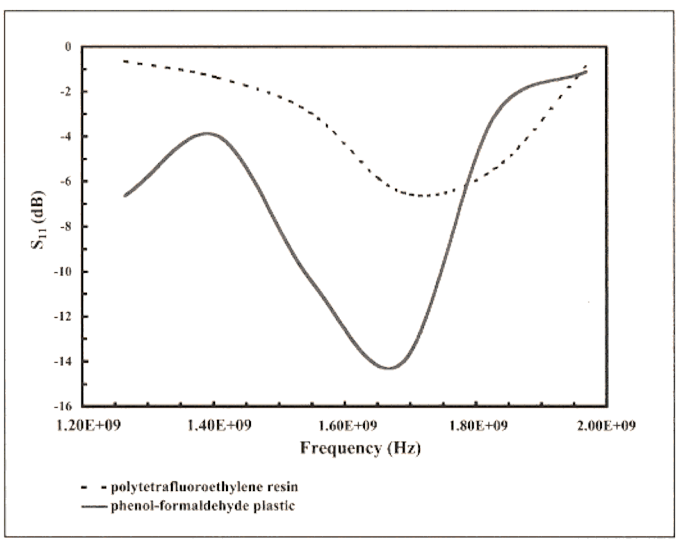

Figure 8 — S_{11} parameter extracted from the transmission line matrix generated signals for two different materials: polytetrafluoroethylene resin ($\varepsilon_r = 5$) and phenol-formaldehyde plastic ($\varepsilon_r = 2$).

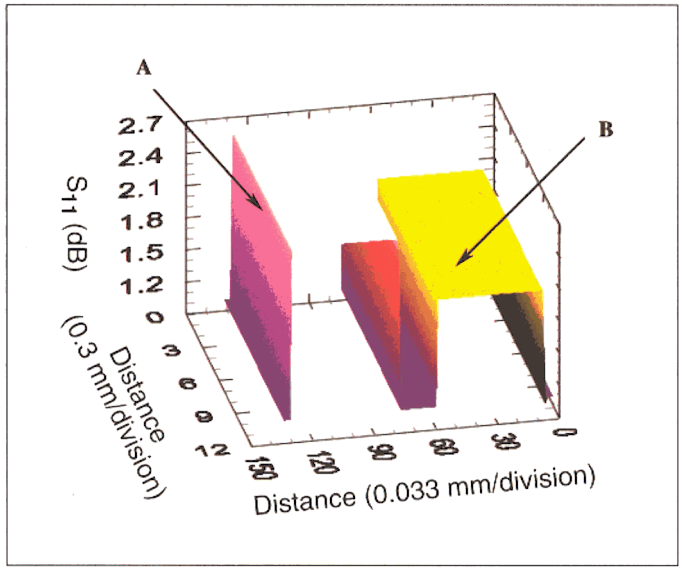

Figure 9 — Results of the numerical scanning for two pieces of dielectric (A = polytetrafluoroethylene resin; B = phenol-formaldehyde plastic) with a 0.561 mm (0.02 in.) gap between them.

CONCLUSIONS

A numerical model for scanning microwave microscopy was implemented. The model is based on the transmission line matrix algorithm. The results shown in this paper demonstrate that the models can be applied to the dimensional characterization of structures with different electric permittivities. The scanning process was also implemented in the numerical model. The results obtained show that the numerical model can be run in parallel with an experimental investigation, allowing a better characterization of reflectors detected by microwave microscopy.

The models developed here can be applied as they are or, depending on requirements and on user capabilities, a few improvements can be easily performed:

- improvement of user interface (a computer aided design interfacing will decrease the amount of resources used in boundary coordinate generation)
- implementation of models described in this paper in a parallel computing configuration will significantly enlarge the capabilities of the numerical models proposed in this work and significantly decrease the computing time. This time was determined to be 162 s for a transmission line matrix model having 3 375 000 nodes (150 by 150 by 150) and running on a computer.

ACKNOWLEDGMENTS

This work was supported in part by the ASNT Fellowship Award. Our special thanks go to the reviewers — without their pertinent suggestions this article would not have been possible.

REFERENCES

Akhtarzad, S. and P.B. Johns, " Numerical Solution of Lossy Waveguides," *Electronics Letters*, Vol. 10, No. 15, 1974, pp. 309-311.

Akhtarzad, S. and P.B. Johns, "Solution of Maxwell's Equations in Three

Space Dimensions and Time by the TLM Method of Numerical Analysis," *Proceedings of the Institution of Electrical Engineers*, Vol. 122, No. 12, December 1975, pp. 1344-1348.

Braemeller, A. and M.N. John, *Practical Diakoptics for Electrical Networks*, London, Chapman and Hall, 1969.

Brewitt-Taylor, C.R. and P.B. Johns, "On the Construction and Numerical Solution of Transmission-line and Lumped Network Models of Maxwell's Equations," *International Journal for Numerical Methods in Engineering*, Vol. 15, 1980, pp. 13-30.

Chadwick, E., P. Bettess and O. Laghrouche, "Diffraction of Short Waves Modeled Using New Mapped Wave Envelope Finite and Infinite Elements," *International Journal for Numerical Methods in Engineering*, Vol. 45, 1999, pp. 335-354.

Ciocan, R., *Numerical Models for Elastic and Electromagnetic Waves Propagation with Applications to Nondestructive Characterization of Materials*, PhD Dissertation, University of Akron, August 2003.

Hoefer, W.J.R. and P.M. So, *The Electromagnetic Wave Simulator: A Dynamic Visual Electromagnetic Laboratory Based on the Two-dimensional TLM Method*, New York, John Wiley & Sons, 1993.

Ida, N., *Developments in Electromagnetic Theory and Applications:* Vol. 10, *Microwave NDT*, Dordrecht, Netherlands, Kluwer Academic Publishers, 1992.

Ida, N., *Numerical Modeling for Electromagnetic Non-destructive Evaluation*, London, Chapman & Hall, 1995.

Ida, N., *Engineering Electromagnetics*, New York, Springer Verlag, 2000.

Johns, P.B. "The Solution of Inhomogeneous Waveguide Problems Using a Transmission-line Matrix," *Transactions on Microwave Theory and Techniques*, Vol. MTT-22, No. 3, 1974, pp. 209-215.

Johns, P.B. "New Symmetrical Condensed Node for Three-dimensional Solution of Electromagnetic-wave Problems by TLM," *Electronics Letters*, Vol. 22, No. 3, 1986, pp. 162-164.

Johns, P.B. "A Symmetrical Condensed Node for the TLM Method," *IEEE Transaction on Microwave Theory and Techniques*, Vol. MTT-35, No. 4, 1987, pp. 370-377.

Johns, P.B. and R.L. Beurle, "Numerical Solution of Two-dimensional Scattering Problems Using a Transmission-line Matrix," *Proceedings of IEEE*, Vol. 118, No. 9, 1971, pp. 1203-1209.

Kagawa, Y., T. Tsuchiya, B. Fujii and K. Fujioka, "Discrete Huygens Model Approach to Sound Wave Propagation," *Journal of Sound and Vibration*, Vol. 218, No. 3, 1998, pp. 419-444.

Livesay, D.E. and K.M. Chen, "Electromagnetic Fields Induced Inside Arbitrarily Shaped Biological Samples," *IEEE Transactions on Microwave Theory Technology*, Vol. MTT-22, No. 12, 1974, pp. 1273-1280.

Paul, J. and C. Christopoulos, "Generalized Material Models in TLM — Part 3: Materials with Nonlinear Properties," *IEEE Transactions on Antennas and Propagation*, Vol. 50, No. 7, 2002, pp. 997-1004.

Sadiku, M.N.O. and C.N. Obiozor, "A Comparison of Finite Difference Time-domain (FDTD) and Transmission-line Modeling (TLM) Methods," *Proceedings of the IEEE SoutheastCon 2000*, Nashville, Tennessee, IEEE, 7-9 April 2000, pp. 19–22.

Yee, K.S., "Numerical Solution of Initial Boundary Value Problems Involving Maxwell's Equation in Isotropic Media," *IEEE Transactions on Antennas and Propagation*, Vol. 14, No. 3, 1966, pp. 302-307.

Zoughi, R., *Microwave Non-destructive Testing and Evaluation Principles*, Dordrecht, Netherlands, Kluwer Academic Publishers, 2000.